文章编号：1001 -9014(2019)05-0554-05

DOI:10. 11972/j. issn. 1001-9014. 2019. 05. 002

The effect of Mn doping on the interband transition and band tail absorption characteristics of Mn:(Pb, Sr)TiO_3 ferroelectric thin films

LI Yan-Qing, WU Man, YANG Jing*

(Key Laboratory of Polar Materials and Devices, Ministry of Education, Department of Electronic, East China Normal University, Shanghai 200241, China)

Abstract: Mn composition dependence of optical properties, especially interband electronic transition and band tail absorption behaviors, in Mn doped (Pb, Sr)TiO_3 (PST) films were investigated by transmittance spectroscopy. The optical parameters of Mn doped PST films in transparent region were evaluated by Cauchy model. The decrease of optical band gap and the expansion of the band tail states with the increasing of Mn dopant amount were observed. The shrinkage of optical band gap is attributed to lowering the bottom of conduction bands by Mn 3d orbitals and the decrease of lattice constant in Mn doped PST films. Meanwhile, the random occupation of Mn ion and the increase of oxygen vacancy after Mn doping are the main causes for the expansion of localized states in band tails.

Key words: ferroelectric films, electronic band structure, optical properties, band tails

PACS: 77. 80. - e, 71. 20. -b, 78. 20. -e

锰掺杂对钛酸锶铅铁电薄膜带-带跃迁和带尾吸收特性的影响

李延青, 吴 曼, 杨 静*

(华东师范大学电子科学系 极化材料与器件教育部重点实验室,上海 200241)

摘要:通过透射光谱研究了锰掺杂量对钛酸锶铅铁电薄膜光学特性尤其是带-带跃迁和带尾吸收特性的影响,并利用柯西色散关系获得了光学透明区的光学常数.研究表明:随着锰掺杂量的增加,钛酸锶铅铁电薄膜的禁带宽度减小而带尾能增加.禁带宽度随锰掺杂的收缩可以归因为锰3d轨道降低了导带底的能级及掺杂后晶格的减小.掺杂锰离子的随机占位和非等价掺杂后氧空位浓度的增加则是导致局域带尾态拓宽的主要原因.

关 键 词:铁电薄膜;电子能带结构;光学特性;带尾

中图分类号:O469 **文献标识码**:A

Introduction

In view of excellent ferroelectric properties, high dielectric constant and great dielectric tunability, ferroelectric (Pb, Sr)TiO_3 (PST) films possess considerable potential applications in a variety of microelectronic-devices, including dynamic random access memories (DRAMs), ferroelectric random access memories (FeRAMs) and microwave tunable devices, etc [1-7]. Apart from these excellent electrical properties, (Pb, Sr)TiO_3 films unfold outstanding electro-optical and photoluminescence features as well. For instance, nonlinear optical response, i. e., the intensive second harmonic generation effect has been found in PST/(001)MgO epitaxial films [8]. Ambika et al. also investigated the optical nonlinearity of PST films in the visible region using the open aperture z-scan technique [9]. The evidence that the third order nonlinear absorption is dependent on ferroelectric

Received date: 2019- 03- 02, **revised date**: 2019- 07- 02 **收稿日期**:2019- 03- 02,**修回日期**:2019- 07- 02

Foundation items: supported by the Natural Science Foundation of China (61574058, 61674058)

Biography: LI Yan-Qing(1993-), female, Weifang, Shandong, master. Research area involves oxide functional materials and physical characterizations. E-mail: yanqingli93@163. com

* **Corresponding author**: jyang@ee. ecnu. edu. cn

polarization was observed. And the value of third order nonlinear absorption (β) was obtained to be 10^{-7}m/W. Utilizing ferroelectric PST film based tunable co-planar waveguide, second and third harmonics generation were produced for a fundamental at centimeter wavelengths [10]. Pyroelectric coefficient p of PST ceramics were evaluated to be $10^{-3}C/m^2K$ and showed good infrared sensitiveness [11]. In addition, nano-crystalline PST films and PST nanotubes exhibited the room temperature tunable blue-green photoluminescence under UV excitation with intense emission bands centered at the range from 350-450 nm, and emission centers can be tuned by changing the Pb content[12-13]. The above mentioned nonlinear optical, infrared response and photoluminescence of PST can be regarded as a candidate for the related photoelectric devices, such as photoelectric modulator, infrared sensors at room temperature, flat panel display devices, the integrated light emission devices, co-planar waveguide and so on.

In general, the proper element doping at A, B sites in ferroelectrics is an effective method to further optimize ferroelectric, dielectric and optical properties. In our previous work, it is found that the ferroelectric and dielectric properties of PST films can be greatly improve by Mn doping [14-15]. However, the issue that Mn composition dependence of optical characteristics of Mn: PST film is still an open topic. Understanding the Mn doping effects on optical properties, especially fundamental and band tail absorption behaviors is in favor of design and optimization of integrated optics, but also provides physics nature about doping modulated electronic energy band structure and localized band tail states. In this study, the transmittance spectroscopy of a series of Mn doped $Pb_{0.5}Sr_{0.5}TiO_3$ films at room temperature are presented. And Mn composition dependence of interband electronic transition and band tail absorption behaviors are investigated.

1 Experimental details

A series of 1, 2.5, 5, 10 mol% Mn doped $Pb_{0.5}Sr_{0.5}TiO_3$ (PSMT1, PSMT2.5, PSMT5, PSMT10) films with 300 nm thickness were prepared on sapphire substrate by chemical solution deposition [14-17]. The precursor solution was spin-coated on sapphire substrates. Then it was dried at 200 ℃ for 3min, heated at 400 ℃ for 3min, annealed at 650 ℃ for 5 min by a RTA furnace in air. The x-ray diffraction (XRD) was preformed for phase identification by a Rigaku-D/MAX3C diffractometer with Cu-Kα radiation at 40 kV. The XRD results show that the present films were pure perovskite structure polycrystalline [14-17]. The transmittance spectroscopy was measured with a double beam spectrophotometer (Perkin Elmer UV/VIS Lambda 2S) at the range from 1 to 5 eV.

2 Results and Discussions

Figure1 shows the transmittance spectroscopy of PSMT films at the range from 1 to 5 eV. In general, from low energy to high energy range, the spectrum is composed of three regions: (I) a transparent oscillating region, (II) a low transmittance region and (III) a fundamental absorption region. In transparent region, due to the multi-reflectance between the film and substrate, the Fabry-Pérot interference patterns are observed in low energy region (<3 eV). It can be seen that the number of Fabry-Pérot interference patterns decreases with Mn doping amount increasing, owing to less transparent in heavily doped PSMT samples. Similar phenomenon was also be reported in Co:$BaTiO_3$ films [18]. Low transmittance region is usually attributed to band tail absorption. The transmittance becomes sharper with the decrease of Mn dopant, which implies the density of localized band tail states rise with introducing Mn into PST lattices. In fundamental absorption region, the interband electronic transition between conduction and valence bands occurs. Therefore, the incidence photons were absorbed by the films totally, leading the transmittance to be zero. As the insets of Fig. 1 shown, the edge of fundamental absorption shift to low energy end, i. e. a red shift comes to being with the increasing of Mn doping. It suggests that Mn doping has influence on the energy band structure and form localized band tail in band gap.

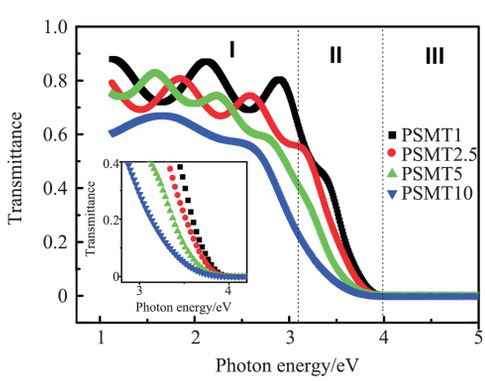


Fig. 1 The transmittance spectroscopy of PSMT films with Mn content 1%, 2.5%, 5% and 10% at photon energy range from 1 to 5 eV. The inset is enlarging scale of transmittance spectroscopy in absorption region

图1 掺杂Mn含量为1%、2.5%、5%和10%的PSMT薄膜在1-5 eV光子能量范围内的透射光谱. 插图是放大的吸收区透射光谱

In transparent region, a three-layered structure (air/film/substrate) was used to fit the transmittance spectroscopy for refraction index of PSMT films [18]. The dielectric function of dielectric layer is descried by Cauchy dispersion relation [19]:

$$n = a + b/\lambda^2 + c/\lambda^4, \quad (1)$$

where n is the refraction index, a, b, c are fitting parameters, λ is incident wavelength. Figure 2(a), (b) and (c) show that the measured data are in consistent with the model fitting results in PSMT1, PSMT2.5 and PSMT5 films. And obtained refraction index of PSMT films is present in Fig. 2 (d), (e) and (f). However, because of less transparency, the fitting with Cauchy dis-

persion relation can not applied in PSMT10. Refraction index of the present films is increasing, when the incidence photon energy becomes stronger. This is a typical dispersion relation of ferroelectric films in transparent region. Generally, in transparent region, the dispersion behavior can be depicted by single oscillator Sellmeier model [20],

$$n(\lambda)^2 - 1 = S_0\lambda_0/[1-(\lambda_0/\lambda)^2] \quad . \quad (2)$$

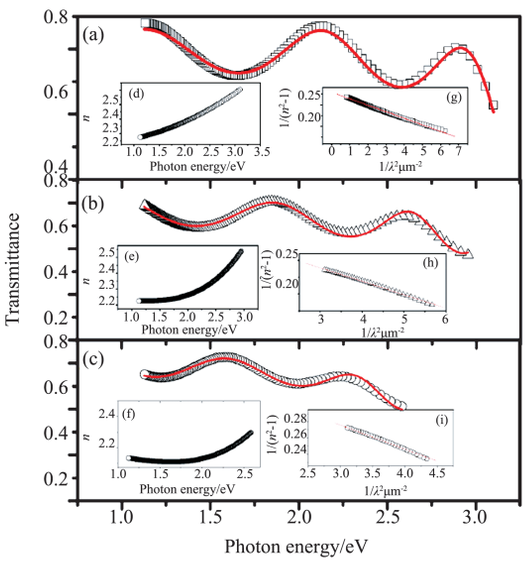


Fig. 2 Experimental (symbols) and calculated (solid lines) data of PSMT films with Mn content (a) 1%, (b) 2.5% and (c) 5% in transparent region. The refractive index (n) and of PSMT films with Mn content (d) 1%, (e) 2.5% and (f) 5% as a function of the photon energy. $1/(n^2-1)$ vs. $1/\lambda^2$ plots of of PSMT films with Mn content (g) 1%, (h) 2.5% and (i) 5%. The solid line is the fitting of the experimental data with a single oscillator model

图2 Mn掺杂量为(a) 1%、(b) 2.5%和(c) 5%的PSMT薄膜在透明区域透射光谱的实验值(符号)和计算值(实线)数据；Mn含量为(d) 1%、(e) 2.5%和(f) 5%的PSMT薄膜的折射率(n)与光子能量的函数关系；Mn含量为(g) 1%, (h) 2.5%和(i) 5% PSMT薄膜中$1/(n^2-1)$与$1/\lambda^2$的关系图

Where λ_0 is an average oscillator position and oscillator energy $E_0=hc/e\lambda_0$, S_0 is an average oscillator strength. $1/(n^2-1)$ vs. $1/\lambda_2$ plots with linear fittings of Sellmeier model are displayed in Fig. 2(g), (h) and (i). And E_0 is obtained to be 5.43, 4.76 and 4.27 eV, S_0 is 0.67, 0.50 and 0.33 $\times10^{14}$ m^{-2} for PSMT1, PSMT2.5 and PSMT5 films, respectively, which are accord with those value in $(Bi, La)_4Ti_3O_{12}$ films[21] and $SrTiO_3$[20]. The transitions between critical points (CP) in high energy region are usually regarded as a single oscillator, which contribute to dielectric dispersion in transparent region[18]. In Ti based perovskite oxides, the higher CP transitions of (A_1-A_2) are scribed to the transition between X_5,- X_5 energy levels and the value of transition energy is 4-5eV[22], which is in agreement with this case and the origin of dielectric dispersion. It can be found that the oscillator energy and strength become weaker with Mn doping, which reveals that high energy CP transition energy decreases and Mn doping alters PST electronic energy band structure. It is in consistent with the above mentioned results about transmittance spectroscopy.

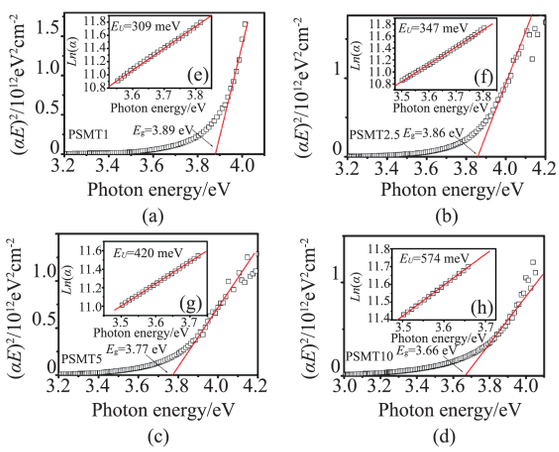


Fig. 3 Variations of $(\alpha E)^2$ changing with the photon energy are used to determine the optical band gap of the PSMT films with Mn content (a) 1%, (b) 2.5%, (c) 5% and (d) 10%. The insets are the exponential absorption coefficient as a function of the photon energy below the band gap energy

图3 $(\alpha E)^2$随光子能量变化而发生的变化，其中Mn含量(a) 1%、(b) 2.5%、(c) 5%和(d) 10%. 插图是低于带隙能量区域内吸收系数的自然指数函数与光子能量的关系

In absorption region, absorption coefficient α is are derived form $\alpha=ln(1/T)/d$ (T is transmittance and d is film thickness) to determine the optical band gap of the PMST films[23]. Usually, in fundamental absorption region ($E>E_g^{opt}$), Tauc's power law can describe the incident photon energy E dependence of the absorption coefficient. There are two case: (1) for the direct interband transition between the valence and conduction bands, $\alpha \propto (E-E_g^{opt})^{1/2}/E$, and (2) for the indirect interband transition, $\alpha \propto (E-E_g^{opt})^2/E$, where E_g^{opt} is optical band gap (OBG)[24]. Good linear fittings of the relations between E and $(\alpha E)^2$ can be shown in Fig. 3(a), (b), (c) and (d), which indicates direct interband transition between the conduction and valence bands in Mn doped PST films. The E_g^{opt} is evaluated to be about 3.89, 3.86, 3.77 and 3.66 eV for PSMT1, PSMT2.5, PSMT5 and PSMT10 films, respectively, which is litter less than that of pure PST films[16]. The Mn composition dependence of optical band gap is shown in Fig. 4. Similar to the decrease of high energy CP transitions as the above mentioned, it is found that optical band gap undergoes shrinkage when Mn content increases, which follows the red-shift of the fundamental absorption edge in transmittance spectroscopy. Moreover, the relation of op-

tical band gap and Mn dopant amount is approximately linear, just as the description of Vegard's law[25]. In Pb-TiO_3-based perovskite ferroelectrics, the upper structure of valence bands mainly comes from O 2*p* orbitals, while the lower laying of conduction bands origins from Ti 3*d* orbitals. Because of crystalline field effect in Ti-O octahedra, Ti 3*d* conduction bands split into lower energy threefold degenerate t_{2g} and higher energy two-fold degenerate Ti 3*d* e_g subbands. Therefore, the lowest laying of conduction bands arises from Ti 3*d* t_{2g} orbitals. The gap of O 2*p* and Ti 3*d* t_{2g} states would be optical band gap and the value of the gap is near 4 eV[26]. Therefore, the optical band gap comes from the interband transition between upper laying of O 2*p* orbitals and lower laying of Ti 3*d* t_{2g} orbitals. Introducing Mn ions into B site of PST lattices, lower enengy Mn 3*d* orbitals partly replace Ti 3*d* t_{2g} orbitals, which can lead to the gradual decline of the lowest laying in conduction bands and the shrinkage of OBG[25], but also influences the hybridization strength between the Ti 3*d*-O 2*p* orbitals and Mn 3*d*-O 2*p* orbitals, and therefore decreases the high energy CP transition. On the other hand, the lattice constant is also a critical cause for OBG. Basing on Harrison model[27], OBG can be determined by

$$E_g = \varepsilon_C - \varepsilon_V - 2\sqrt{2}\,(V_{pp\sigma} + V_{pp\pi}) \quad , \quad (3)$$

where ε_c is lowest laying of conduction band, ε_V is top of conduction band, $V_{pp\sigma}$ and $V_{pp\pi}$ is σ and π bonding energies of O 2*p* orbital, respectively. The last term varies with interatomic distance (t), in terms of

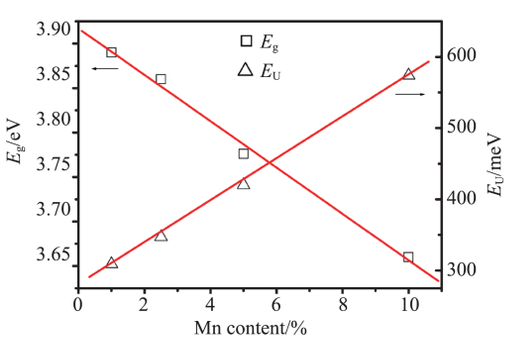


Fig. 4　Mn composition dependence of optical band gap and Urbach band tail energy of PSMT film. The solid line is the linear fitting of the experimental data

图4　PSMT薄膜的光学带隙和Urbach带尾能量与Mn组分的依赖关系,实线是实验数据的线性拟合

$$V_{pp\sigma} + V_{pp\pi} = (\eta_{pp\sigma} + \eta_{pp\pi})(h^2/m)t^{-f} \quad , \quad (4)$$

where $\eta_{pp\sigma}$, $\eta_{pp\pi}$ and f are dimensionless coefficients, m is the electron mass and h is Planck constant. As reported by Yang *et al*, the lattice parameter of PST films decreases after the Mn doping[15]. The decrease of interatomic distance can enhance the value of $V_{pp\sigma} + V_{pp\pi}$ and in turn contribute to the decrease of OGB.

Note that the absorption coefficient increases gradually when the incidence photon energy is increasing below OGB (~3.4-3.8eV), as the above motioned band tail absorption in a low transmittance region. This weak band tail absorption can be suggested as the electronic transition among the extended bands and the localized band tail states. Usually, this weak band tails absorption behavior obeys Urbach rule, which is described by $\alpha \propto exp(E/E_U)$[28], where Urbach band tail energy (E_U) is the width of band tails of local states. The inset of Fig. 3 (a), (b), (c) and (d) show that the band tail absorption yields Urbach law well and Urbach band tail energy is obtained to be 309, 347, 420 and 574 meV for PSMT1, PSMT2.5, PSMT5 and PSMT10 films (in Fig. 4), respectively, which are larger than that of pure PST films (245 meV)[16]. Urbach band tail energy increases with more Mn amount doping into PST films, which means the width of band tails of local states increasing. The localized states of Urbach tail are usually resulted from the thermal fluctuation disorder (electron-phonon interaction) or/and the structural disorder in lattices[16,29]. Obviously, doping induced Urbach tail states can be interpreted as the structural disorder, which is resulted from the impurities, defects e.g., oxygen vacancy or Pb vacancy and grain boundaries[16]. In present case, firstly, Mn dopant ions occupy B site Ti ions randomly, which leads to the disorder of the lattices. Moreover, as an acceptor doping, with the Mn^{2+} dopant amount increasingly entering into Ti^{4+} site, the more concentration of oxygen vacancy with two positive charges will generate to keep electrical neutral of the whole film system[14-15]. This process can be described by

$$MnO \rightarrow Mn_{Ti}^{''} + 1/2O_2 + V_o^{\cdot\cdot} \quad . \quad (5)$$

The increase of oxygen vacancy further deteriorates the structural disorder. Therefore, random occupation of Mn ion and the increase of oxygen vacancy after Mn doping are the main causes for the expansion of localized states in band tails.

3　Conclusions

In summary, Mn doping induced the decrease of interband transition energy and the expansions of the band tail states were observed. Lowering the bottom of conduction bands by Mn 3*d* orbitals and the decrease of lattice constant in Mn doped PST films contribute to the shrinkage of optical band gap. And the random occupation of Mn ion and the increase of oxygen vacancy after Mn doping are the main causes for the expansion of localized states in band tails.

References

[1] Naik V M, Haddad D, Naik R, *et al*. Phase transitional studies of polycrystalline $Pb_{0.4}Sr_{0.6}TiO_3$ films using Raman scattering [J]. *Journal of Applied Physics*, 2003, **93**(3): 1731-1734.
[2] Wang J L, Lai Y S, Chiou B S, *et al*. Study on fatigue and breakdown properties of Pt/(Pb, Sr) TiO_3/Pt capacitors [J]. *Journal of Physics: Condensed Matter*, 2006, **18**(46): 10457-10467.
[3] Yang J, Chu J H, Shen M R. Analysis of diffuse phase transition and relaxorlike behaviors in $Pb_{0.5}Sr_{0.5}TiO_3Pb_{0.5}Sr_{0.5}TiO_3$ films through dc electric-field dependence of dielectric response [J]. *Applied Physics Letters*, 2007, **90**(24): 242908.
[4] Liu S W, Lin Y, Weaver J, *et al*. High-dielectric-tunability of ferroelectric (Pb, Sr)TiO_3 thin films on (001) $LaAlO_3$ [J]. *Applied Physics Letters*, 2004, **85**(15): 3202-3204.

[5] Liu S W, Weaver J, Yuan Z, *et al*. Epitaxial nature and anisotropic dielectric properties of (Pb,Sr)TiO_3 thin films on $NdGaO_3$ substrates [J]. *Applied Physics Letters*, 2005, **86**(14):142902.
[6] Jiang J C, Meletis E I, Yuan Z, *et al*. Interface modulated structure of highly epitaxial (Pb,Sr)TiO_3 thin films on (001) MgO [J]. *Applied Physics Letters*, 2007, **90**(5):051904.
[7] Lin Y, Chen X, Liu S W, *et al*. Anisotropic in-plane strains and dielectric properties in (Pb,Sr)TiO_3 thin films on $NdGaO_3$ substrates [J]. *Applied Physics Letters*, 2004, **84**(4):577-579.
[8] Liu S W, Chakhalian J, Xiao M, *et al*. Second harmonic generation and ferroelectric phase transitions in thick and ultrathin $Pb_{0.35}Sr_{0.65}TiO_3$ films on (001) MgO substrates [J]. *Applied Physics Letters*, 2007, **90**(4):042901.
[9] Ambika D, Kumar V, Sandeep C S Suchand, *et al*. Non-linear optical properties of $(Pb_{1-x}Sr_x)TiO_3$ thin films [J]. *Applied Physics B-Lasers and Optics*, 2009, **97**(3): 661-664.
[10] Ponchel F, Burgnies L, Ducatteau D, *et al*. A fully distributed non linear waveguide using (Pb,Sr)TiO_3 thin film: Second and third harmonics generation [J]. *Journal of Applied Physics*, 2013, **114**(19): 194103.
[11] Sun P, Wang M X, Sun T, *et al*. Preparation and characteristics of the infrared sensitive ferroelectric ceramics $(Pb_{1-x}Sr_x)TiO_3$ [J]. *Ferroelectrics*, 2001,**264**(1-4):1839-1842.
[12] Luo L, Ren H Z, Tang X G, *et al*. Room temperature tunable blue-green luminescence in nanocrystalline $(Pb_{1-x}Sr_x)TiO_3$ thin film grown on yttrium-doped zirconia substrate [J]. *Journal of Applied Physics*, 2008, **104**(4):043514.
[13] Jiang Y P, Tang X G, Zhou Y C, *et al*. Structure and composition-dependent optical properties of $(Pb_xSr_{1-x})TiO_3$ (x=0.4, 0.6) nanotube arrays [J]. *Progress in Natural Science Materials International*, 2011, **21**(3): 198-204.
[14] Yang J, Meng X J, Shen M R, *et al*. Hopping conduction and low-frequency dielectric relaxation in 5 mol% Mn doped (Pb,Sr)TiO_3 films [J]. *Journal of Applied Physics*, 2008, **104**(10):104113.
[15] Yang J, Meng X J, Shen M R, *et al*. Effects of Mn doping on dielectric and ferroelectric properties of (Pb,Sr)TiO_3 films on (111) Pt/Ti/SiO_2/Si substrates [J]. *Journal of Applied Physics*, 2009, **106**(9): 094108.
[16] Yang J, Gao Y Q, Huang Z M, *et al*. Dielectric functions of ferroelectric $Pb_{0.5}Sr_{0.5}TiO_3$ film determined by transmittance spectroscopy [J]. *Journal of Physics D-Applied Physics*, 2009, **42**(21):215403.
[17] Yang J, Gao Y Q, Wu J, *et al*. Temperature dependent optical properties of Mn doped (Pb,Sr)TiO_3 ferroelectric films in absorption region: Electron - phonon interaction [J]. *Journal of Applied Physics*, 2010, **108**(11):114102.
[18] Hu Z G, Li Y W, Zhu M, *et al*. Composition dependence of dielectric function in ferroelectric $BaCo_xTi_{1-x}O_3$ films grown on quartz substrates by transmittance spectra [J]. *Applied Physics Letters*, 2008, **92**(8):081904.
[19] Liu S W, Jolly S, Xiao M, *et al*. Domain microstructures and ferroelectric phase transition in $Pb_{0.35}Sr_{0.65}TiO_3$ films studied by second harmonic generation in reflection geometry [J]. *Journal of Applied Physics*, 2007, **101**(10):104118.
[20] DiDomenico M, Wemple S H. Oxygen-Octahedra Ferroelectrics. I. Theory of Electro- optical and Nonlinear optical Effects [J]. *Journal of Applied Physics*, 1969, **40**(2):720.
[21] Hu Z G, Wang G S, Huang Z M, *et al*. Investigations on optical properties of very thin $Bi_{3.25}La_{0.75}Ti_3O_{12}$ ferroelectric thin films [J]. *Journal of Infrared and Millimeter Waves*, 2003, **22**(4):256-260.
[22] Cardona M. Optical Properties and Band Structure of $SrTiO_3$ and $BaTiO_3$ [J]. *Physical Review*, 1965, **140**(2A): 651-655.
[23] Leng W J, Yang C R, Ji H, *et al*. Linear and nonlinear optical properties of (Pb,La)(Zr,Ti)O_3 ferroelectric thin films grown by radio-frequency magnetron sputtering [J]. *Journal of Physics D-Applied Physics*, 2007, **40**(4):1206-1210.
[24] Tauc J. Optical properties of non-crystalline solids [J]. *Optical Properties of Solids*, 1972:277-313.
[25] Li Y W, Sun J L, Meng X J, *et al*. Structural and optical properties of $Ba(Co_x,Ti_{1-x})O_3$ thin films fabricated by sol-gel process [J]. *Applied Physics Letters*, 2004, **85**(11):1964-1966.
[26] Cohen R E. Origin of ferroelectricity in perovskite oxides [J]. *Nature*, 1992, **358**(6382):136-138.
[27] Zhu J S, Lu X M, Jiang W, *et al*. Optical study on the size effects in $BaTiO_3$ thin films [J]. *Journal of Applied Physics*, 1997, **81**(3): 1392-1395.
[28] Hu Z G, Li Y W, Zhu M, *et al*. Microstructural and optical investigations of sol-gel derived ferroelectric $BaTiO_3$ nanocrystalline films determined by spectroscopic ellipsometry [J]. *Physics Letters A*, 2008, **372**(24):4521-4526.
[29] Beaudoin M, DeVries A J G, Johnson S R, *et al*. Optical absorption edge of semi-insulating GaAs and InP at high temperatures [J]. *Applied Physics Letters*, 1997, **70**(26):3540-3542.